JPET Fast Forward. Published on May 12, 2006 as DOI: 10.1124/jpet.106.105015

High-Glucose-Altered Endothelial Cell Function Involves Both Disruption of Cell-to-Cell Connection and Enhancement of Force Development

***Koji Nobe, Mari Miyatake, Tomoko Sone &**

Kazuo Honda

Department of Pharmacology, School of Pharmaceutical Sciences (K.N., M.M., T.S., K.H.), Showa University, Tokyo 142-0555, Japan

1) Running Title: Alteration of EC functions under high-glucose conditions

2) * Address correspondence to:

Koji Nobe, Ph.D., Department of Pharmacology,

School of Pharmaceutical Sciences, Showa University,

1-5-8 Hatanodai, Shinagawa-ku, Tokyo 142-0555, Japan

Tel: +81-3-3784-8212

Fax: +81-3-3784-3232

E-mail: kojinobe@pharm.showa-u.ac.jp

3) Word Counts:

Text pages: 46 pages

Number of tables: 0

Number of figures: 6

Number of references: 32

Number of words in abstract: 246 words

Number of words in introduction: 652 words

Number of words in discussion: 1499 words

4) List of non-standard abbreviations

ASF, actin stress fiber; $[Ca^{2+}]_i$, intracellular calcium concentration; DG, diacylglycerol; EC, endothelial cells; HG, high glucose; PBS, phosphate-buffered saline; PI, phosphatydylinositol; PKC, protein kinase C; PSS, physiological salt solution; TXA_2, thromboxane A_2; U46619, TXA_2 analogue; VE-CaD, vascular endothelial cadherin.

5) Recommended section

Diabetes

ABSTRACT

Vascular endothelial cells (EC), which regulate vascular tonus, serve as a barrier at the interface of vascular tissue. It is generally believed that alteration of this barrier is correlated with diabetic complications; however, a detailed mechanism has not been elucidated. This study examined alteration of bovine arterial EC functions stimulated by a thromboxane A_2 analogue (U46619) under normal- and high-glucose (HG) conditions. U46619 treatment increased EC layer permeability in time- and dose-dependent fashion. This response initially disrupted calcium-dependent EC-to-EC connections, namely, vascular endothelial cadherin (VE-CaD). Subsequently, EC force development in association with morphological changes was detected employing a re-constituted EC fiber technique, resulting in paracellular hole formation in the EC layer. Thus, we confirmed that U46619-induced enhancement of EC layer permeability involves these sequential steps. Similar trials were performed utilizing a concentration twice that of normal glucose (22.2 mM glucose for 48 hr). This treatment significantly enhanced U46619-induced EC layer permeability; furthermore, increases in both rate of VE-CaD disruption and EC fiber contraction were evident. Inhibition of calcium-independent protein kinase C and diacylglycerol kinase indicated that the glucose-dependent increase in VE-CaD disruption was mediated by a calcium-independent mechanism. Moreover, EC contraction was regulated by a typical calcium-

independent pathway associated with rho kinase and actin stress fiber. Contraction was also enhanced under HG conditions. This investigation revealed that glucose-dependent enhancement of EC layer permeability is related to increases in VE-CaD disruption and EC contraction. Increases in both parameters were mediated by alteration of a calcium-independent pathway.

JPET Fast Forward. Published on May 12, 2006 as DOI: 10.1124/jpet.106.105015
This article has not been copyedited and formatted. The final version may differ from this version.

Introduction

Diabetes mellitus is associated with various types of metabolic vascular dysfunction mediated by sustained elevation of plasma glucose levels (Calles-Escandon and Cipolla, 2001; Ceriello, 2003). In major diabetic complications, including angioneurosis, retinopathy and nephropathy, it is generally accepted that dysfunction of micro-resistant arteries is responsible for perivascular tissue damage (Ostergaard et al., 2005; Yu and Lyons, 2005). Endothelial cells (EC), which regulate vascular tonus via nitric oxide synthesis (Cohen, 2005), serve as a barrier at the interface of vascular tissue (Lum and Malik, 1994). The increase in EC layer permeability in local resistant artery is thought to be an early manifestation of EC barrier dysfunction and its induced diabetic complications. For example, enhancement of EC layer permeability can lead to edema and proliferative diabetic retinopathy (Qaum et al., 2001). Based on this perspective, evidence corresponding to the relationship between alteration of oxidative stress and/or NO synthesis and complications of diabetic hyperglycemia has accumulated (Prabhakar, 2004; Santilli et al., 2004; Niedowicz and Daleke, 2005). In contrast, studies have indicated that glucose-induced enhancement of EC layer permeability is dependent on protein kinase C (PKC) activity in the absence of mediation of the calcium-NO synthesis pathway (Dang et al., 2005). According

to these findings, critical conclusions with respect to alteration of EC function in diabetic hyperglycemia have not been established.

We previously reported that the inflammatory factor thrombin induces enhancement of EC layer permeability (Nobe et al., 2005), which is mediated via a two-step process: 1) Interaction of EC-to-EC adhesion molecules, namely, vascular endothelial cadherin (VE-CaD), was disrupted during the initial stage of thrombin stimulation; cell-to-cell connections were decreased. 2) EC indicated force development (non-muscle contraction) characterized by morphological changes; cell-to-cell distances increased, resulting in the formation of paracellular holes. We concluded that these sequential steps play a central role in alteration of EC layer permeability. To detect EC force development, a re-constituted EC fiber technique was introduced. This EC fiber was re-constituted in a collagen matrix, which made possible detection of absolute force development in cultured EC. Utility of this EC fiber force measurement system revealed that the thrombin-induced responses involved two distinct pathways, which operated as intracellular signaling pathways. Reduced VE-CaD signals were associated with a calcium-dependent pathway, whereas EC contraction was associated with a calcium-independent pathway. However, alterations of these pathways under high-glucose (HG) conditions, as in diabetes, are poorly understood.

We previously demonstrated that EC-replaced mouse aorta (Nobe et al., 2003) and portal vein (Nobe et al., 2004b) contractions were induced by treatment with the thomboxane A_2 (TXA_2) analogue, U46619. These contractions were significantly enhanced under HG conditions; furthermore, intracellular diacylglycerol (DG) level and PKC activity were elevated during this enhancement. Similar changes were also described in other types of tissues (Ramana et al., 2005; Rolo and Palmeira, 2006). We suggested over-acceleration of phosphatidylinositol (PI) turnover as a possible mechanism of enhanced vascular contraction. Incorporated glucose is converted to DG via a *de novo* synthesis pathway under HG conditions; as a result, excess accumulation of DG was believed to be a key step in vascular dysfunction as this situation might lead to activation of PKC. Additionally, similar accumulation of DG was observed. Alteration of this vascular smooth muscle contraction might be associated with diabetic complications. We hypothesized that EC function was also influenced under HG conditions in a manner identical to that of smooth muscle dysfunction. However, alteration of EC function due to U46619 has not been examined. We believe that a thorough understanding of alteration of U46619-induced EC function and its intracellular mechanisms are of utmost importance in order to facilitate the establishment of a new target for care in diabetic complications.

The objective of this investigation was to identify the contribution of extracellular glucose

accumulation to U46619-induced EC layer permeability. Subsequently, the relationships of both VE-CaD response and EC contraction to alteration of EC layer permeability were evaluated as the major mechanisms of diabetic vascular dysfunction.

Materials and Methods

Reagents. Bovine aortic endothelial cells were provided by Dr. S. Shimizu (Dept. of Pathophysiol., Showa Univ., Tokyo). Calf serum and Dulbecco's modified Eagle's medium (DMEM) containing 11.1 mM (2 g/L) glucose were obtained from Life Technologies (Grand Island, NY, USA). Rat tail collagen type-I was procured from Upstate Biotechnology (Lake Placid, NY, USA). Fura-2/AM, BAPTA/AM, Alexa 488-phalloidine and SYTO-17 were acquired from Molecular Probes (Eugene, OR, USA). Thromboxane A_2 analogue (U46619), phospholipase C inhibitor (U73122), and SQ29548 were purchased from Sigma Chemical Co. (St. Louis, MO, USA). Rho kinase inhibitor (Y-27632) and Rottlerin were obtained from Wako Pure Chemical Corporation (Osaka, Japan) and Funakoshi Corporation (Tokyo, Japan), respectively. Vascular endothelial cadherin (VE-CaD) antibody was acquired from Alexis

Biochemicals (Tokyo, Japan). Diacylglycerol (DG) kinase inhibitor, stemphone, was a gift from Mitsubishi Pharma Corporation (Yokohama, Japan). U73122 and U46619, which were dissolved in dimethyl sulfoxide (DMSO) and ethanol, respectively, served as stock solutions. Concentrations of DMSO and ethanol in all solutions in the bathing medium were less than 0.05% (these reagents did not affect mechanical responses). The remaining reagents were dissolved in de-ionized water. All reagent dilutions and reactions were conducted in MOPS-buffered physiological salt solution (PSS) containing (mM) 140 NaCl, 4.7 KCl, 1.2 NaH_2PO_4, 0.02 EDTA, 1.2 $MgSO_4$, 2.5 $CaCl_2$, 11.1 glucose and 20 MOPS (pH 7.4) at 37 ^oC. HG conditions were achieved by addition of sufficient glucose to produce a 22.2 mM (twice that of normal conditions) solution in DMEM and PSS at 37 ^oC for 48 hr.

Cell Culture. EC were cultured in DMEM supplemented with 10% CS. Cells, which were grown on 60-mm dishes in an incubator in an atmosphere of 5% CO_2 and 95% air at 37 ^oC, displayed typical cobblestone morphology. Cells were propagated in 0.05% trypsin and phosphate-buffered saline (PBS) with a split ratio of 1:4 every three days. All experimental data were derived from EC obtained from 7~20 passages.

Preparation of Three-dimensionally Re-constituted Endothelial Cell Fibers (EC fibers). EC fibers were prepared according to Nobe, *et al.*(Nobe et al., 2005). Rat tail collagen (Type-I) solution was neutralized with 0.1 N NaOH in an ice bath. Dispersed cells were suspended in a solution containing 1 X 10^7 cells/mL and 0.5 mg/mL collagen in DMEM. A cell suspension (2 mL) was poured into a specially designed mold (0.8 cm X 5 cm X 0.5 cm deep), which was cut into a layer of silicone rubber in a 60-mm dish, and placed in a CO_2 incubator at 37 ^oC. EC fiber preparations were incubated for three days. In a manner identical to that of the monolayer EC culture, DMEM was exchanged daily.

Measurement of Isometric Force Development in EC Fibers. EC fibers were cut into 5-mm sections and mounted between stainless wire posts with cyanoacrylate glue. One post was fixed, whereas the opposite post was connected to a silicone strain gauge force transducer (model AME801, SensoNor, Horton, Norway). EC fibers were mounted isometrically under resting tension of 20 ± 1.0 μN at 37 ^oC; fibers were bathed in PSS.

Measurement of EC Layer Permeability. EC layer permeability was measured as described previously (Imai-Sasaki et al., 1995; Nobe et al., 2005). Results of BSA permeability of the EC layer

JPET Fast Forward. Published on May 12, 2006 as DOI: 10.1124/jpet.106.105015
This article has not been copyedited and formatted. The final version may differ from this version.

were calculated as "total amount of BSA (μg) / area of EC layer (cm^2)".

Measurement of Intracellular Free Ca^{2+} Concentration ($[Ca^{2+}]_i$). ECs were grown on cover glasses (diameter, 25 mm) placed inside 35-mm dishes. The $[Ca^{2+}]_i$ was measured as described previously (Nobe et al., 2005).

VE-cadherin Immunostaining. VE-cadherin immunostaining was conducted as previously described.(Sandoval et al., 2001)

Labeling of EC Structures and Digital Imaging. To determine the mechanism(s) via which cytoskeletal molecules are affected by stimulators, EC were grown to the third day of post-subconfluence on a cover glass inside 35-mm dishes. Following rinsing of the culture medium with PSS, EC were treated under various conditions at 37 ^oC. The reaction was terminated and fluorescent staining was performed as described previously (Nobe et al., 2005). A digital imaging microscope was utilized to view the stained samples (Bio Rad-MRC600 confocal microscope equipped with a 60X, 1.4 NA

JPET Fast Forward. Published on May 12, 2006 as DOI: 10.1124/jpet.106.105015
This article has not been copyedited and formatted. The final version may differ from this version.

oil immersion objective). Fluorescent images of the samples excited at 488 nm (Alexa 488-Phalloidine) and 568 nm (SYTO-17), and emitting at 504~540 nm and 585~700 nm, respectively, were collected. Digital images were qualified and/or merged with Confocal Assistant (Bio Rad) and Photoshop (Adobe) software.

Statistics and Data Analysis. Data presented in the text and the illustrations are expressed as mean ± S.E.M. The permeability value at each condition was assessed in terms of statistical significance for comparison with appropriate control data employing the analysis of variance techniques. Paired data were utilized when appropriate. P values < 0.01 were considered significant. ANOVA statistical comparisons were performed with the Y-Stat program. For western blot and fluorescent imaging, similar patterns of changes were detected in nearly all samples (> six trials).

Results

U46619-induced Enhancement of EC Responses Under HG Conditions. Confluent cultures of

JPET Fast Forward. Published on May 12, 2006 as DOI: 10.1124/jpet.106.105015
This article has not been copyedited and formatted. The final version may differ from this version.

EC were pre-incubated with normal- and HG-DMEM for 48 hr to assess the effects of extracellular glucose levels on EC function. Penetration of FITC-BSA though the EC layer was measured to identify alterations of EC barrier function (Fig. 1A) in normal- and HG-PSS. Barrier function in the absence of stimulation was maintained during the measurement (1-120 min); moreover, the values did not differ between these glucose concentrations. Values at 60 min were 20.83 ± 0.65 and 26.67 ± 0.75 μg/cm^2 (n=5), respectively. Addition of 10 μM U46619 enhanced EC layer permeability. Meaningful enhancement was first detected from 15 min of stimulation under normal glucose conditions. The sub-maximal value (195.95 ± 8.67 μg/cm^2; n=5) was observed at 60 min. In a manner similar to this response, increases in EC layer permeability were also present under HG conditions; however, the increase was rapid and the response was larger in comparison to that under normal conditions. Significant differences from the value obtained under normal glucose conditions were evident from 5 min of stimulation. The value at 60 min of stimulation was 279.40 ± 3.59 μg/cm^2 (n=5). Increases in EC layer permeability at 60 min were dependent on U46619 concentration (Fig. 1B). Enhancement of permeability under HG conditions was also detected. Differences between normal and HG conditions were apparent at 0.03 μM U46619. EC_{50} values in normal- and HG-PSS were approximately 0.25 and 0.12 μM, respectively. These U46619-induced responses were suppressed by pre-treatment with the

thromboxane A_2 receptor antagonist, SQ29548 (1 μM) (Fig. 1B-inset).

In order to assess the influence of HG treatment on cell-to-cell connections in the EC layer, alteration of vascular endothelial cadherin (VE-CaD) was measured (Fig. 2). In the non-stimulated resting state under normal glucose conditions, the presence of VE-CaD connections was evident (Fig. 2A). VE-CaD signals were detected for more than 90% of cell junction components. U46619 (10 μM) challenge induced disruption of VE-CaD connections in time-dependent fashion. After 60 min of stimulation, VE-CaD signals remained for only 5-10% of cell junctions. Rather, cell-to-cell distances increased and paracellular holes formed after 60 min of stimulation. Pre-incubation of EC under HG conditions did not influence the resting VE-CaD signal (Fig. 2B); however, addition of 10 μM U46619 induced rapid (3 min) disruption of the VE-CaD connections. More than 90% of the signals disappeared during the initial 3-min period. Moreover, formation of paracellular holes was advanced.

To elucidate the mechanisms, effects of a PKC inhibitor (rottlerin) and a DG kinase inhibitor (stemphone) on U46619-induced VE-CaD depression were also examined. In normal-PSS, U46619-induced depression of VE-CaD signals was apparently reduced by pre-treatment with rottlerin and stemphone. In excess of 50% of the original signals remained in the presence of these inhibitors. Similar effects were detected under HG conditions. Advanced VE-CaD depression reached the normal level in

the presence of these inhibitors.

Isometric force development of EC accompanied by morphological changes, i.e., paracellular hole formation, was determined using three-dimensionally re-constituted EC fibers (Fig. 3). EC fibers were pre-incubated in normal- and HG-DMEM for 48 hr in a manner consistent with that of the aforementioned experiments; subsequently, 5-mm sections were mounted on a specially designed isometric force measurement system. The length was increased to match the original fiber length in the mold. Following stress relaxation, the force attained a baseline level of 20.30 ± 0.27 μN (n = 5). Treatment with 10 μM U46619 induced sustained force development in normal glucose-PSS (Fig. 3). This response was time-dependent. Pre-treatment of EC fibers with HG-DMEM slightly increased the non-stimulated resting level (29.30 ± 1.86 μN; n=5). Although U46619 treatment led to an increase in sustained force development, the increase was rapid and the response was large. Maximal force responses, including baseline, to U46619 under normal and HG conditions after the 60-min period were 45.00 ± 1.80 and 63.80 ± 3.14 μN, respectively (n=5). Significant enhancement of U46619-induced force development under HG conditions was observed from 3 min of stimulation. In order to confirm alteration of EC fiber contractility in HG-PSS, increased force value in the initial 5 min of U46619 stimulation was calculated as the “initial rate” (Fig. 3B-inset). This initial rate was significantly elevated from 2.49 ±

JPET Fast Forward. Published on May 12, 2006 as DOI: 10.1124/jpet.106.105015
This article has not been copyedited and formatted. The final version may differ from this version.

0.15 to 4.81 ± 0.32 μN/min (n=5).

These HG-induced alterations of EC responses were dependent on the extracellular glucose concentration and pre-incubation period. In preliminary trials, each condition of extracellular glucose concentration (11.1-33.3 mM) or pre-incubation period (1-96 hr) was challenged in terms of permeability and contraction assays (data not shown). Based on consideration of stability and reproducibility of effects, HG conditions (22.2 mM glucose for 48 hr) were adopted as a chronic HG model in this study.

Intracellular Signaling Mechanisms of HG-induced Enhancement of EC Responses. To establish the intracellular mechanisms governing U46619-induced EC responses, several key factors of cellular functions were investigated. A general intracellular factor, intracellular calcium concentration ($[Ca^{2+}]_i$) was measured with the calcium indicator, Fura-2, loaded into the EC (Fig. 4A). Pre-treatment of EC with HG-DMEM did not affect resting $[Ca^{2+}]_i$. Averages of $[Ca^{2+}]_i$ in randomly selected non-stimulated 30 cells under normal and HG conditions were 41.17 ± 1.11 and 43.33 ± 2.20 nM, respectively. In normal glucose-PSS, treatment of EC with 10 μM U46619 led to a rapid increase in $[Ca^{2+}]_i$. The maximal peak level, which was 153.5 ± 8.17 nM, was attained only 42 sec after the stimulation. This response returned to the resting level during the fourth minute of stimulation. A similar transient increase in $[Ca^{2+}]_i$ was observed in EC pre-treated with HG-DMEM-pre-treated EC. Patterns of

JPET Fast Forward. Published on May 12, 2006 as DOI: 10.1124/jpet.106.105015
This article has not been copyedited and formatted. The final version may differ from this version.

changes and the maximal level (163.00 ± 3.59 nM) also overlapped with the response in normal-PSS. EC were pre-treated with the intracellular calcium inhibitor, BAPTA/AM, for 30 min prior to U46619 treatment (Fig. 4A-inset). The transient increases in $[Ca^{2+}]_i$ under normal and HG conditions were suppressed (34.83 ± 1.70 and 39.67 ± 2.54 nM, respectively) without affecting resting levels. Differences between normal- and HG-PSS could not be detected in intracellular calcium measurements.

The effects of some kinds of inhibitors in terms of enhancement of EC layer permeability under HG conditions were examined (Fig. 4B). U46619-induced enhancement of EC layer permeability under normal and HG conditions was confirmed (195.95 ± 6.67 and 279.40 ± 3.59 μg/cm^2, respectively; n=5). In a manner identical to that of Fig. 4A, the EC layer was pre-treated with 1 μM BAPTA/AM for 30 min. Significant inhibition of permeability in normal- and HG-PSS was detected (81.70 ± 4.05 and 150.40 ± 10.75 μg/cm^2, respectively; n=5); however, differences between the two glucose conditions remained. Other key factors of EC function, particularly the association of PKC and DG kinase with EC layer permeability, were also evaluated employing rottlerin and stemphone as specific inhibitors. These substances display a tendency to inhibit calcium-independent isoforms of PKC or DG kinase. Treatment with 1 μM rottlerin suppressed U46619-induced EC-layer permeability without affecting resting levels under both glucose conditions (44.92 ± 3.10 and 47.92 ± 5.60 μg/cm^2, respectively; n=5). Similar effects

were observed following treatment with stemphone (53.78 ± 1.71 and 54.10 ± 3.10 μg/cm^2, respectively; n=5). These inhibitors also suppressed differences between normal and HG conditions. Inhibitory effects were also evident upon introduction of calphostin C or R59022 (data not shown). These conventional inhibitors cannot distinguish between calcium-dependent and –independent isoforms.

The roles of rho and the rho kinase pathway in U46619-induced EC fiber contraction were examined in order to discern alteration of sustained function following completion of intracellular calcium events under HG conditions (Fig. 5). The rho kinase inhibitor, Y27632 (1 μM), markedly reduced U46619-induced force development under normal and HG conditions (Fig. 5A, 5B). The maximal force developments in the presence of Y27632 were 22.50 ± 0.83 and 23.80 ± 1.13 μN (n=5), respectively. Differences between normal and HG conditions were suppressed. Although the initial rate of the response was also diminished, significant differences between normal- and HG-PSS remained (Fig. 5C). As a downstream of the Rho-Rho kinase pathway, actin stress fiber (ASF) formation was measured (Fig. 5D). ASF reconstitution was induced by treatment with 10 μM U46619 in time-dependent fashion. The pattern of the time-course was similar to the response in EC fiber force development. This response was suppressed upon pre-treatment with 1 μM Y27632. Under HG conditions, enhanced U46619-induced ASF formation was apparent; however, it was inhibited in the presence of Y27632. Paracellular hole

formation was also reduced following Y27632 treatment in normal- and HG-PSS.

Discussion

The current investigation examined EC barrier dysfunction under HG conditions. Experiments involved enhancement of both VE-CaD disruption and EC contraction. Several studies have shown that TXA_2 plays an important role in diabetic vascular complications (Davi et al., 1990; Kobayashi et al., 2005). This importance is based mainly on the low concentration (0.1-30 nM) of the TXA_2 analogue, U46619, necessary to induce significant contraction in diabetic models (Pfister et al., 2004). We also documented 10 nM U46619-induced sub-maximal contractions in mouse aorta (Nobe et al., 2003), portal vein (Nobe et al., 2004a) and porcine coronary artery (Nobe and Paul, 2001). However, this range of U46619 concentrations did not markedly influence EC layer permeability (Teixeira et al., 1995; Nobe et al., 2005). Although these results indicated that the physiological concentration of TXA_2 might not affect EC function, the effect under abnormal conditions is unknown. In actuality, these findings revealed that some types of prostanoids, including TXA_2, are produced locally in excess in instances of inflammatory

diseases (Tonshoff et al., 1992). Diabetic hyperglycemia and inflammatory conditions were presumed in this investigation; therefore, higher concentrations (10 nM-30 μM) of U46619 were introduced. TXA_2 receptor-mediated time- and dose-dependent increases in EC layer permeability were detected within this range (Fig. 1). Moreover, previous reports demonstrated that similar levels of TXA_2 induced enhancement in EC layer permeability in other types of EC (Chang and Ohara, 1993), which was consistent with the response obtained in this study. During U46619 treatment, cell-to-cell connector, e.g., VE-CaD, signals were reduced (Fig. 2) and significant increases in EC fiber contraction (Fig. 3) were observed. These responses were similar to those of thrombin stimulation (Nobe et al., 2005), which suggested that thrombin and U46619 induced both disruption of VE-CaD signals and EC contraction, which were mediated by common mechanisms in EC layer permeability. Contraction of EC in U46619-induced enhancement of EC layer permeability was identified in this investigation; however, it appears that this phenomenon preferentially accompanies hyperglycemia rather than solely elevating TXA_2 in diabetes.

Based on this perspective, alteration of U46619-induced EC responses under HG conditions was considered in order to evaluate EC dysfunction in diabetic complications. Under HG conditions, EC were pre-incubated with medium containing 22.2 mM glucose (DMEM and MOPS-PSS) for 48 hr in

JPET Fast Forward. Published on May 12, 2006 as DOI: 10.1124/jpet.106.105015
This article has not been copyedited and formatted. The final version may differ from this version.

accordance with our previous experiments involving vascular smooth muscle tissue (Nobe et al., 2004a; Nobe et al., 2004b). We previously confirmed that HG medium treatment induced neither hyperosmolar nor non-selective actions (data not shown). Moreover, HG-induced responses in this investigation were sub-maximum; higher concentration (22.2 mM <) and long-term treatment (48 hr <) were not dependent on increases in EC response (data not shown). Reports appearing in the literature indicate that viability and cellular functions of rataortic EC were maintained under similar HG conditions (Lee et al., 2004). These results suggested that similar HG treatment of EC led to enhancement of non-stimulated basal EC layer permeability; however, meaningful differences were not detected in the current study. Although several possibilities exist regarding these differences (EC species, culture conditions, etc.), a critical cause remains unknown.

Under HG conditions, U466619-induced EC layer permeability was enhanced (Fig. 1). EC layer permeability was not derived from enhancement of TXA_2 receptor sensitivity (Fig. 1B-*inset*). Similar enhancement was not evident under high-sucrose conditions (11.1 mM sucrose added to normal medium for 48 hr); alteration of EC layer permeability was caused by an increase in extracellular glucose concentration. In our preliminary measurements, enhanced EC layer permeability in HG medium was recovered upon restoration of EC to normal glucose medium, although it was slow and incomplete (data

JPET Fast Forward. Published on May 12, 2006 as DOI: 10.1124/jpet.106.105015
This article has not been copyedited and formatted. The final version may differ from this version.

not shown). This recovery rate appears to be dependent on glucose concentration and pre-treatment period. This finding may suggest that sustained elevation of blood glucose level leads to a long-term EC disorder.

In order to elucidate the mechanism(s) governing EC layer alteration under HG conditions, both VE-CaD signal (Fig. 2) and EC contraction (Fig. 3) were examined; moreover, alterations of both parameters were observed. These findings indicated that these alterations are directly attributable to enhancement of EC layer permeability. However, questions regarding intracellular mechanisms associated with extracellular glucose level abound. A major contractile factor, $[Ca^{2+}]_i$ was measured during U46619 stimulation in normal and HG mediums. A transient increase in intracellular calcium response was detected; however, the response was not dependent on extracellular glucose concentration (Fig. 4A). Inhibition of the transient increase in $[Ca^{2+}]_i$ by BAPTA/AM did not suppress the EC layer response. Importantly, significant differences between the two glucose conditions remained in the presence of BAPTA/AM (Fig. 4B). We hypothesized that extracellular glucose influenced a point downstream of the calcium signaling pathway or the calcium-independent signaling pathway. Downstream of the calcium signaling pathway, the association of PKC and DG kinase activities with EC function was assessed consequent to over-activation of PKC and DG kinase, which leads to dysfunction

of vascular smooth muscle cells mediated by over-acceleration of PI-turnover. Each treatment with PKC and DG kinase inhibitor suppressed reduction of U46619-induced EC layer permeability as well as differences between normal and HG mediums (Fig. 4B). As a result of these treatments, differences of VE-CaD signals under normal and HG conditions were also diminished (Fig. 2). These findings suggested that elevated extracellular glucose accelerated PI-turnover mediated by PKC-DG kinase activities; additionally, it induced enhancement of the disruption rate of VE-CaD signals (Fig. 6A, 6B).

Interestingly, inhibitors of PKC (rottlerin) and DG kinase (stemphone) possess selectivity for calcium-independent isoforms (De Witt et al., 2001; Nobe et al., 2004a). We hypothesized that the elevated response of EC under HG conditions is mediated by the calcium-independent PKC-DG kinase pathway. We previously reported that incorporated glucose under HG conditions is converted to a non-natural species of DG via a *de novo* synthesis pathway in rat and mouse vascular smooth muscle cells (Nobe et al., 2004a). As a preliminary measurement, we also measured a [^{14}C]DG formation from extracellular [^{14}C]glucose as similar as our previous report (Nobe et al., 2004b). Treatment of the EC with the [^{14}C]glucose-contained HG-PSS significantly enhanced the [^{14}C]DG formation (262% of normal glucose). This enhancement was maintained in the U46619 stimulation (296% of normal glucose). These results indicated a possibility that the DG formation under HG condition was increased without mediating

phospholipase C. Depended on the DG formation from extracellular glucose, total PKC activity was also increased (data not shown). Other investigators documented similar findings (Marignani et al., 1996; Deacon et al., 2002). In EC, data suggested that the elevation in extracellular glucose induces accumulation of the non-natural DG species as well as PKC activation; furthermore, this phenomenon might contribute to the rapid disruption of VE-CaD signals. Several groups reported that b-catenin, a regulatory factor of VE-CaD, is phosphorylated by PKC (Berk et al., 1995; Sandoval et al., 2001), which leads to an un-coupling of VE-CaD connections (Fig. 6A, B); in contrast, other researchers noted that activation of PKC is not involved in VE-CaD regulation (Vouret-Craviari et al., 1998). Regulatory mechanisms of this point remain incomplete; however, the current results are consistent with those of the former investigations.

In our preliminary trials employing the non-selective PKC inhibitor, calphostin C (1 μM pre-treatment for 10 min), and the calcium-dependent PKC inhibitor, Gö6976 (1 μM pre-treatment for 10 min), U46619-induced VE-CaD disruption was detected exclusively following calphostin C application (data not shown). These results supported the possibility that increased disruption of VE-CaD under HG conditions is mediated by a calcium-independent PKC-DG kinase pathway. Transient elevation of $[Ca^{2+}]_i$ induced by U46619 contributed to activation of PI-turnover; however, the $[Ca^{2+}]_i$ increase may not

participate in extracellular glucose-dependent over-activation of the PKC-DG kinase pathway. The initial rate of U46619-induced EC contraction served as a marker of initial EC response. Moreover, this rate was enhanced under HG conditions (Fig. 3B-inset); additionally, this enhancement remained despite the presence of a rho kinase inhibitor (Fig. 5C). These findings were also suggestive of the importance of regulation of VE-CaD disruption by the calcium-independent PKC-DG kinase pathway.

We previously noted that disruption of VE-CaD connections was insufficient for the thrombin-induced increase in EC layer permeability (Nobe et al., 2005). It was suggested that EC contraction also contributed to the increase in EC layer permeability consequent to paracellular holes. Rho and the rho kinase-mediated calcium-independent signaling pathway were involved; furthermore, rho and the rho kinase pathway may contribute to U46619-indcued EC contraction. In U46619-induced EC contractions, initial rate and maximal force developments were significantly enhanced under HG conditions (Fig. 3). These responses were followed by ASF formation (Fig. 5D). Pre-treatment with a rho kinase inhibitor markedly reduced maximal contraction and ASF formation without suppressing differences in initial rates between normal and HG conditions (Fig. 5). These findings revealed that rho/rho kinase-mediated ASF re-arrangements are correlated with U46619-induced EC contraction (Fig. 6C). Enhancement of this contraction under HG conditions is derived from over-activation of this pathway. Inhibition of

paracellular hole formation by Y27632 also provided evidence regarding the importance of this pathway (Fig. 5D). Additionally, inhibition of EC-layer permeability by Y27632 was also confirmed under same condition of Fig. 5D (data not shown). Alteration of EC layer permeability under HG conditions might entail an increase in VE-CaD signal disruption in the initial period as well as a secondary step consisting of over-contraction of EC.

The current investigation demonstrated that dysfunction of the EC layer under HG conditions, as in diabetes, is associated with both the rapid, extracellular glucose-dependent disruption of VE-CaD connections during the initial period as well as with the ensuing rho kinase-ASF-mediated EC over-contraction. In the initial phase, accumulation of the glucose-derived non-natural DG species stimulated calcium-independent PKC and DG kinase isoforms, which might lead to an increase in VE-CaD disruption. In the contraction phase, the rho-rho kinase pathway was also activated by elevation of extracellular glucose level, which results in paracellular hole formation via over-contraction of EC. This sequential process contributes to enhancement of EC layer permeability under HG conditions.

Despite the findings of the present study, important and difficult questions remain in terms of detailed regulatory mechanism(s) governing VE-CaD disruption by activated PKC in HG medium and direct or indirect correlation of extracellular glucose level with the rho-rho kinase pathway. Although these points

require additional examination, this investigation confirmed that elevation of extracellular glucose level in diabetes influences vascular smooth muscle function as well as EC layer function. These dysfunctions in major components of vascular tissue might lead to diabetic complications mediated by excessive vascular permeability. In order to treat EC dysfunction, normalization of this process appears to be essential. Artificial regulation of these steps might be a suitable therapeutic target for diabetic vascular dysfunction.

In conclusion, exposure of the EC layer to TXA_2 under diabetic-like HG conditions induces both suppression of cell-to-cell connections via VE-CaD and enhancement of paracellular hole formation due to EC over-contraction. These extracellular glucose- dependent responses may induce diabetic complications via enhanced EC layer permeability.

Acknowledgments

The authors wish to thank to Dr. S. Shimizu (Showa Univ., Tokyo, Japan) who provided the EC.

References

Berk BC, Corson MA, Peterson TE and Tseng H (1995) Protein kinases as mediators of fluid shear stress stimulated signal transduction in endothelial cells: a hypothesis for calcium-dependent and calcium-independent events activated by flow. *J Biomech* **28**:1439-1450.

Calles-Escandon J and Cipolla M (2001) Diabetes and endothelial dysfunction: a clinical perspective. *Endocr Rev* **22**:36-52.

Ceriello A (2003) The possible role of postprandial hyperglycaemia in the pathogenesis of diabetic complications. *Diabetologia* **46 Suppl 1**:M9-16.

Chang SW and Ohara N (1993) Increased pulmonary vascular permeability in rats with biliary cirrhosis: role of thromboxane A2. *Am J Physiol* **264**:L245-252.

Cohen RA (2005) Role of nitric oxide in diabetic complications. *Am J Ther* **12**:499-502.

Dang L, Seale JP and Qu X (2005) High glucose-induced human umbilical vein endothelial cell hyperpermeability is dependent on protein kinase C activation and independent of the Ca2+-nitric oxide signalling pathway. *Clin Exp Pharmacol Physiol* **32**:771-776.

Davi G, Catalano I, Averna M, Notarbartolo A, Strano A, Ciabattoni G and Patrono C (1990) Thromboxane biosynthesis and platelet function in type II diabetes mellitus. *N Engl J Med* **322**:1769-1774.

De Witt BJ, Kaye AD, Ibrahim IN, Bivalacqua TJ, D'Souza FM, Banister RE, Arif AS and Nossaman BD (2001) Effects of PKC isozyme inhibitors on constrictor responses in the feline pulmonary vascular bed. *Am J Physiol Lung Cell Mol Physiol* **280**:L50-57.

Deacon EM, Pettitt TR, Webb P, Cross T, Chahal H, Wakelam MJ and Lord JM (2002) Generation of diacylglycerol molecular species through the cell cycle: a role for 1-stearoyl, 2-arachidonyl glycerol in the activation of nuclear protein kinase C-betaII at G2/M. *J Cell Sci* **115**:983-989.

Imai-Sasaki R, Kainoh M, Ogawa Y, Ohmori E, Asai Y and Nakadate T (1995) Inhibition by beraprost sodium of thrombin-induced increase in endothelial macromolecular permeability. *Prostaglandins Leukot Essent Fatty Acids* **53**:103-108.

Kobayashi T, Matsumoto T and Kamata K (2005) IGF-I-induced enhancement of contractile response in organ-cultured aortae from diabetic rats is mediated by sustained thromboxane A2 release from endothelial cells. *J Endocrinol* **186**:367-376.

Lee HZ, Yeh FT and Wu CH (2004) The effect of elevated extracellular glucose on adherens junction

proteins in cultured rat heart endothelial cells. *Life Sci* **74**:2085-2096.

Lum H and Malik AB (1994) Regulation of vascular endothelial barrier function. *Am J Physiol* **267**:L223-241.

Marignani PA, Epand RM and Sebaldt RJ (1996) Acyl chain dependence of diacylglycerol activation of protein kinase C activity in vitro. *Biochem Biophys Res Commun* **225**:469-473.

Niedowicz DM and Daleke DL (2005) The role of oxidative stress in diabetic complications. *Cell Biochem Biophys* **43**:289-330.

Nobe K, Miyatake M, Nobe H, Sakai Y, Takashima J and Momose K (2004a) Novel diacylglycerol kinase inhibitor selectively suppressed an U46619-induced enhancement of mouse portal vein contraction under high glucose conditions. *Br J Pharmacol* **143**:166-178.

Nobe K and Paul RJ (2001) Distinct pathways of Ca(2+) sensitization in porcine coronary artery: effects of Rho-related kinase and protein kinase C inhibition on force and intracellular Ca(2+). *Circ Res* **88**:1283-1290.

Nobe K, Sone T, Paul RJ and Honda K (2005) Thrombin-induced force development in vascular endothelial cells: contribution to alteration of permeability mediated by calcium-dependent and -independent pathways. *J Pharmacol Sci* **99**:252-263.

Nobe K, Suzuki H, Nobe H, Sakai Y and Momose K (2003) High-glucose enhances a thromboxane A2-induced aortic contraction mediated by an alteration of phosphatidylinositol turnover. *J Pharmacol Sci* **92**:267-282.

Nobe K, Suzuki H, Sakai Y, Nobe H, Paul RJ and Momose K (2004b) Glucose-dependent enhancement of spontaneous phasic contraction is suppressed in diabetic mouse portal vein: association with diacylglycerol-protein kinase C pathway. *J Pharmacol Exp Ther* **309**:1263-1272.

Ostergaard J, Hansen TK, Thiel S and Flyvbjerg A (2005) Complement activation and diabetic vascular complications. *Clin Chim Acta* **361**:10-19.

Pfister SL, Pratt PE, Kurian J and Campbell WB (2004) Glibenclamide inhibits thromboxane-mediated vasoconstriction by thromboxane receptor blockade. *Vascul Pharmacol* **40**:285-292.

Prabhakar SS (2004) Role of nitric oxide in diabetic nephropathy. *Semin Nephrol* **24**:333-344.

Qaum T, Xu Q, Joussen AM, Clemens MW, Qin W, Miyamoto K, Hassessian H, Wiegand SJ, Rudge J, Yancopoulos GD and Adamis AP (2001) VEGF-initiated blood-retinal barrier breakdown in early diabetes. *Invest Ophthalmol Vis Sci* **42**:2408-2413.

Ramana KV, Friedrich B, Tammali R, West MB, Bhatnagar A and Srivastava SK (2005) Requirement of aldose reductase for the hyperglycemic activation of protein kinase C and formation of

diacylglycerol in vascular smooth muscle cells. *Diabetes* **54**:818-829.

Rolo AP and Palmeira CM (2006) Diabetes and mitochondrial function: Role of hyperglycemia and oxidative stress. *Toxicol Appl Pharmacol*.

Sandoval R, Malik AB, Minshall RD, Kouklis P, Ellis CA and Tiruppathi C (2001) Ca(2+) signalling and PKCalpha activate increased endothelial permeability by disassembly of VE-cadherin junctions. *J Physiol* **533**:433-445.

Santilli F, Cipollone F, Mezzetti A and Chiarelli F (2004) The role of nitric oxide in the development of diabetic angiopathy. *Horm Metab Res* **36**:319-335.

Teixeira CF, Farmer P, Laporte J, Jancar S and Sirois P (1995) Increased permeability of bovine aortic endothelial cell monolayers in response to a thromboxane A2-mimetic. *Agents Actions Suppl* **45**:47-52.

Tonshoff B, Momper R, Schweer H, Scharer K and Seyberth HW (1992) Increased biosynthesis of vasoactive prostanoids in Schonlein-Henoch purpura. *Pediatr Res* **32**:137-140.

Vouret-Craviari V, Boquet P, Pouyssegur J and Van Obberghen-Schilling E (1998) Regulation of the actin cytoskeleton by thrombin in human endothelial cells: role of Rho proteins in endothelial barrier function. *Mol Biol Cell* **9**:2639-2653.

Yu Y and Lyons TJ (2005) A lethal tetrad in diabetes: hyperglycemia, dyslipidemia, oxidative stress, and endothelial dysfunction. *Am J Med Sci* **330**:227-232.

Footnotes

This work was supported to in part by a Showa University Grant-in Aid for Innovative Collaborative Research Projects and a Special Research Grant-in Aid for Development of Characteristic Education from the Japanese Ministry of Education, Culture Sports, Science and Technology (K. H.).

JPET Fast Forward. Published on May 12, 2006 as DOI: 10.1124/jpet.106.105015
This article has not been copyedited and formatted. The final version may differ from this version.

Legends for Figures

Fig. 1. U46619-induced enhancement of EC layer permeability in HG-PSS. EC were cultured on collagen-coated mesh (5 mm^2) plates. EC were pre-incubated under normal (open and bright columns) and HG (closed and dark columns) conditions 48 hr prior to the assay. EC were rinsed with MOPS-PSS; subsequently, U46619 was introduced at 37^oC under each condition (A, 10 μM U46619 for indicated periods; B, indicated concentration for 60 min). Glucose conditions were maintained during the rise and the stimulation. Some samples underwent pre-treatment with 1 μM SQ29548 for 15 min, followed by the introduction of 10 μM U46619 for 60 min (B-inset). Simultaneously, 25 μM FITC-BSA containing 2% BSA was added for the reactions. Upon completion of the reaction, medium in the lower chamber was collected and the total amount of BSA (μg) was determined based on FITC-BSA fluorescence levels as described in "Methods". Results are indicated as BSA permeability (μg/cm^2). Each point represents the mean ± SEM from at least 5 independent determinations. * $p<0.01$ vs. non-stimulated control, # $p<0.01$ vs. Normal-PSS and † $p<0.01$ vs. U46619-response.

Fig. 2. U46619-induced alteration of VE-CaD connections in HG-PSS. EC grown to confluence on cover glasses were incubated with normal (A) and HG (B) medium for 48 hr. U46619 (10 μM) was introduced for indicated periods. A PKC inhibitor (rottlerin; 1 μM) and a DG kinase inhibitor (stemphone; 1μM) were pre-incubated for 10 min prior to 10 μM U46619 stimulation (60 min). Reactions were terminated with 4% paraformaldehyde. Samples were permeabilized with 0.1% triton-X100. Cells were exposed to anti-VE-CaD antibody and SYTO-17 for nuclear staining as described in "Methods". Samples were visualized with Alexa-fluora-488 anti-rabbit IgG. Fluorescent images of Alexa fluora-488 (green) and SYTO-17 (red) were collected employing confocal laser microscopy. Scale bar = 30 μm.

Fig. 3. U46619-induced force development in EC fibers under normal and HG conditions. EC fibers were re-constituted from cultured EC with native type-I collagen. These EC fibers were pre-incubated under normal (open and bright columns) and HG (closed and dark columns) conditions 48 hr prior to the assay. The fiber (5 mm) was mounted on a specially designed force measurement apparatus with a resting tension of 20 μN. Following confirmation of stable resting tension, 10 μM U46619 was added at 37^{o}C for indicated periods (B). A typical record of force development is presented (A). The increase in

JPET Fast Forward. Published on May 12, 2006 as DOI: 10.1124/jpet.106.105015
This article has not been copyedited and formatted. The final version may differ from this version.

force development in the initial 5-min period of U46619 stimulation was calculated as an initial rate (μN/min; B-inset). Each value represents the mean ± SEM of 5 independent determinations. * $p<0.01$ vs. responses in normal-PSS.

Fig. 4. Effects of signal transduction inhibitors on U46619-induced increases in intracellular calcium concentration (A) and EC layer permeability (B). EC were grown on a cover glass to sub-confluency; subsequently, cells were incubated with normal (open and bright columns) and HG (closed and dark columns) medium for 48 hr. Fura-2/AM (5 μM) was introduced to the EC at room temperature for 60 min to determine intracellular free Ca^{2+} concentration. Fluorescent images of fura-2 were collected using a fluorescence image system (Argus/HiSCA system) (excitation: 340 and 380 nm; emission: 510 nm). Following confirmation of stable resting levels, 10 μM U46619 was added. Each line indicates the average of typical cellular responses in the same microscopic field. Peak calcium responses were summarized (A-inset). BAPTA/AM (1 μM) was introduced 30 min prior to U46619 addition. In a manner similar to that of the calcium measurement, EC-layer permeability was measured as described in Fig. 1. EC layers pre-treated with normal and HG medium-pre-treated EC layers were incubated in the presence or absence of 1 μM BAPTA/AM for 30 min. PKC (rottlerin; 1 μM) and DG kinase

(stemphone; 1 μM) inhibitors were pre-incubated for 10 min. Subsequently, 10 μM U46619 was added for 60 min. Each value is the mean ± SEM from at least 5 independent determinations. * $p<0.01$ vs. non-treated control and # $p<0.01$ vs. U46619.

Fig. 5. Effect of Rho kinase inhibitor on U46619-induced force development and cytoskeletal re-arrangements. EC fibers were pre-incubated under normal (bright columns) and HG (dark columns) conditions; subsequently, isometric force developments were detected in a manner similar to that of Fig. 3. A Rho kinase inhibitor (Y27632; 1 μM) was introduced 10 min prior to U46619 treatment. Typical records of force development (A) and maximal levels (B) are presented. The increase in force development during the initial 5 min of U46619 stimulation was calculated as an initial rate (μN/min; C). Similar trials were conducted using cultured EC on a cover glass for measurement of ASF formation (D). Reactions were terminated with 4% paraformaldehyde. Samples were permeabilized with 0.1% triton-X100. ASF (green) and nuclei (red) were stained with Alexa fluora-488 phalloidine and SYTO-17, respectively, as described in "Methods". Scale bar = 30 μm.

Fig. 6. Alternation of EC responses under HG conditions. Intracellular mechanisms in U46619-stimulated EC under HG conditions are illustrated. Abbreviations: ASF, actin stress fiber; α-Cat, α-catenin; β-Cat, β-catenin; Ca, calcium ion; DG, diacylglycerol; DGK, diacylglycerol kinase; FAU, focal adhesion units; GLT, glucose transporter; Gq, Gq-protein; p120, p120 protein; PKC, protein kinase C; Rho-K, rho kinase; TX-R, thromboxane receptor; VE-CaD, vascular endothelial cadherin. HG-induced events are depicted with red marks and arrows.

JPET Fast Forward. Published on May 12, 2006 as DOI: 10.1124/jpet.106.105015
This article has not been copyedited and formatted. The final version may differ from this version.

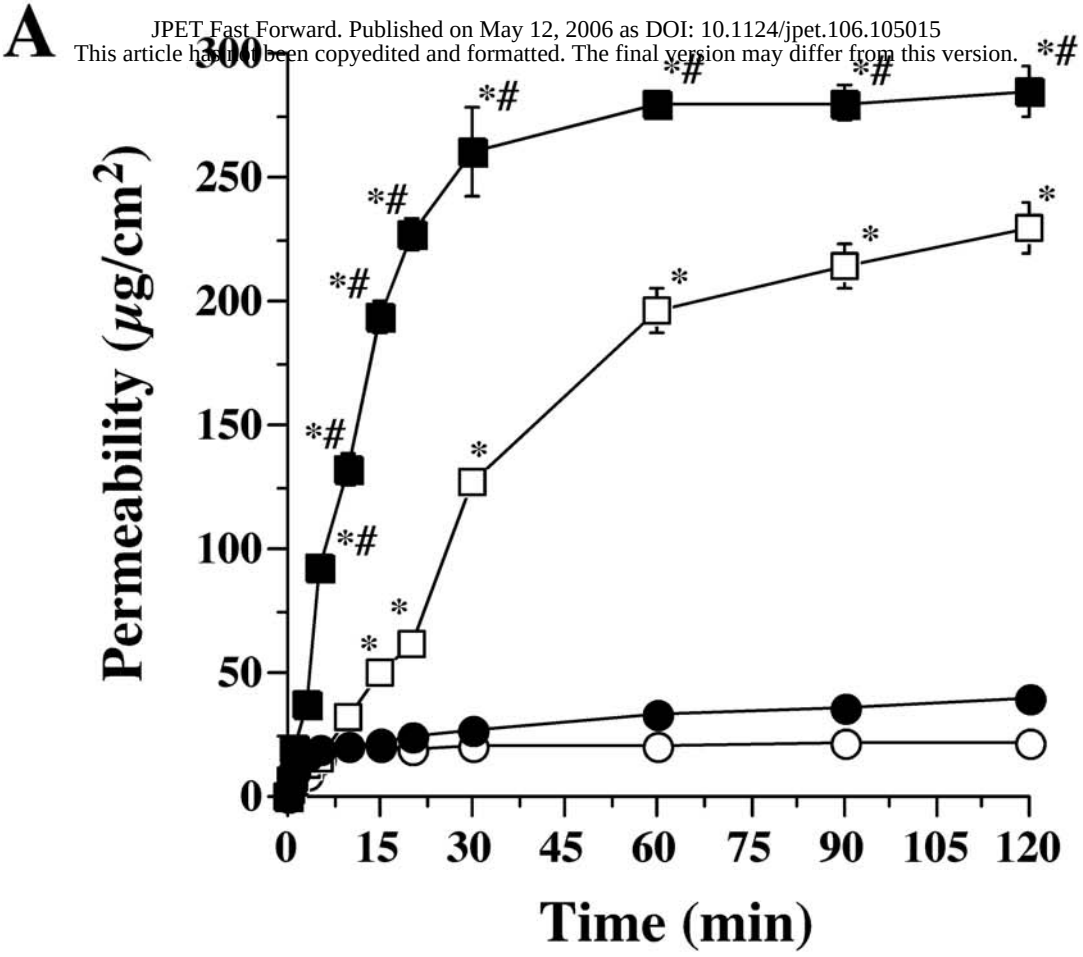

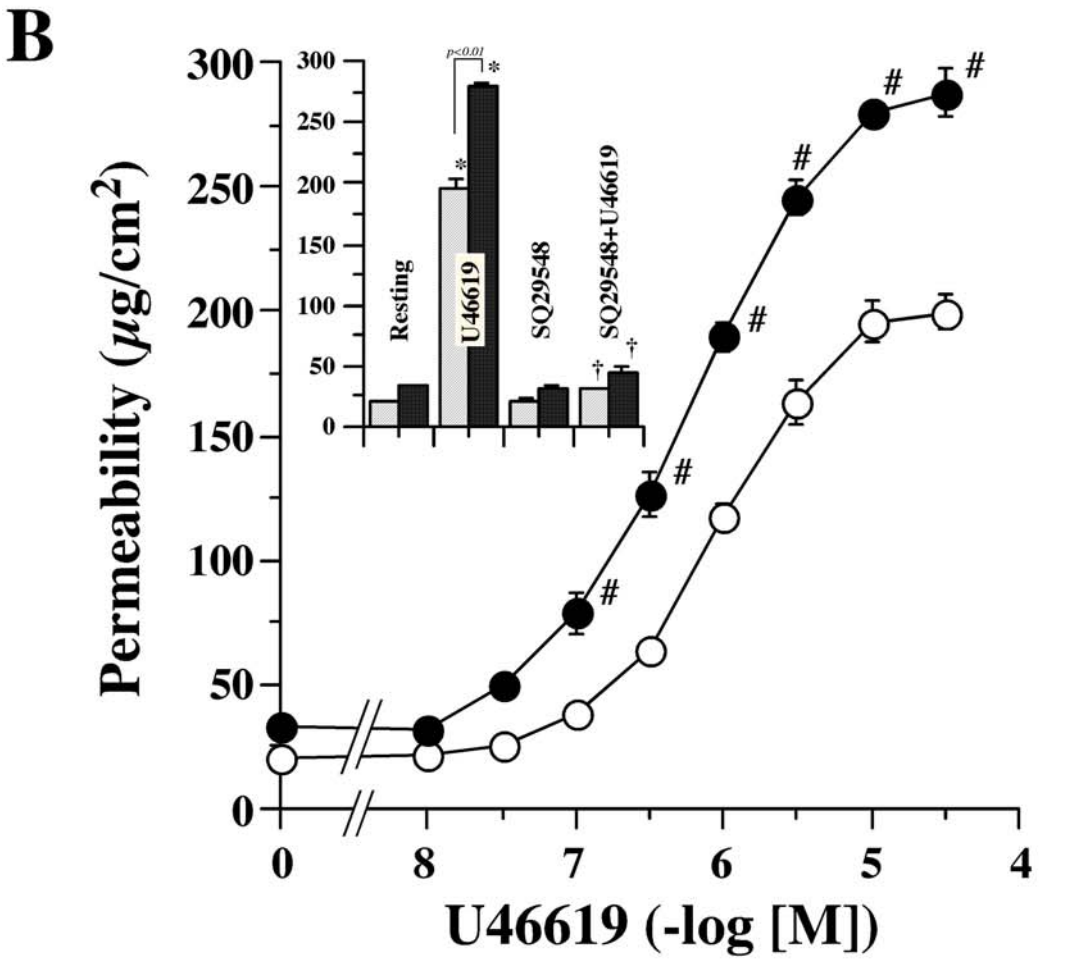

Figure 1

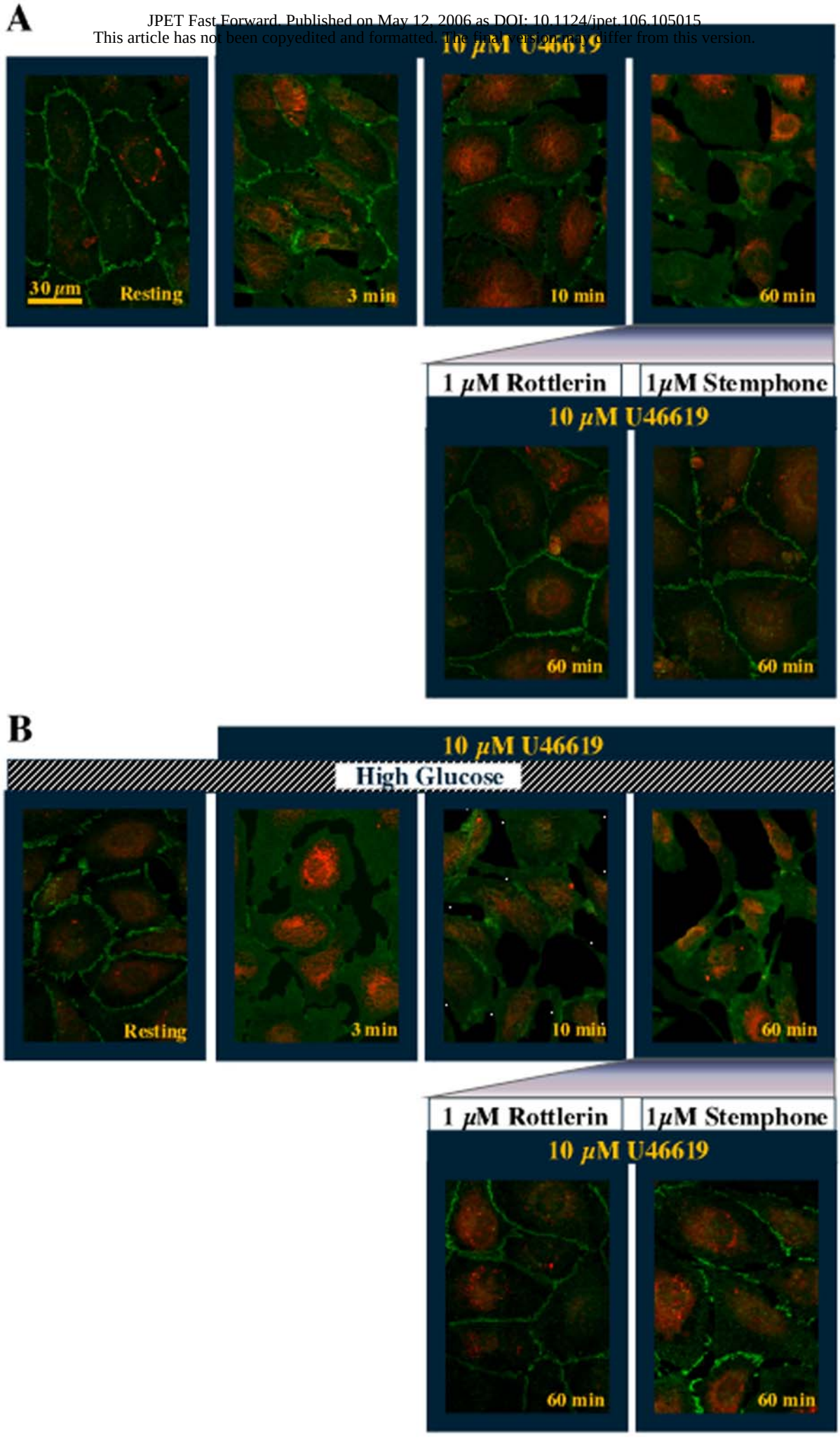

Figure 2

JPET Fast Forward. Published on May 12, 2006 as DOI: 10.1124/jpet.106.105015
This article has not been copyedited and formatted. The final version may differ from this version.

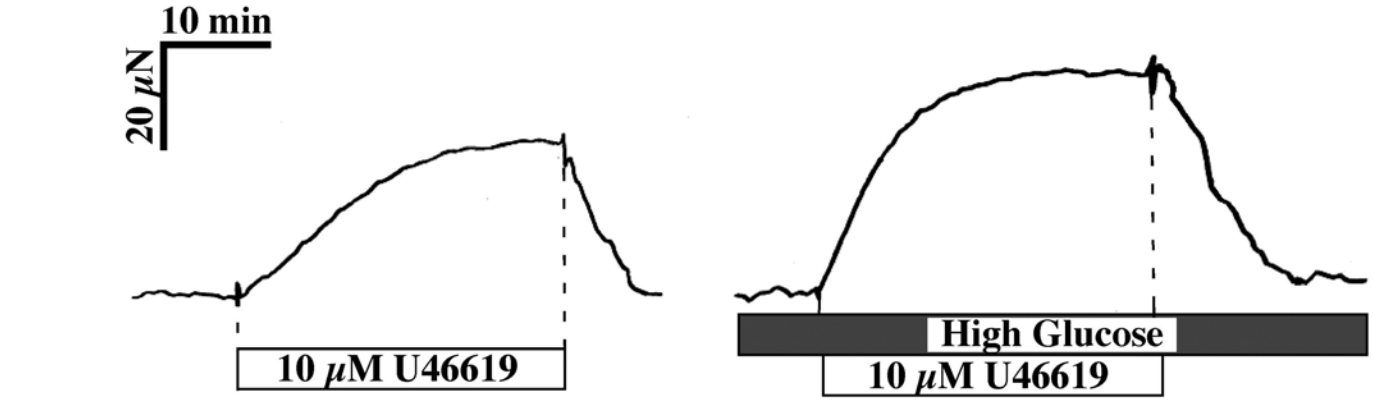

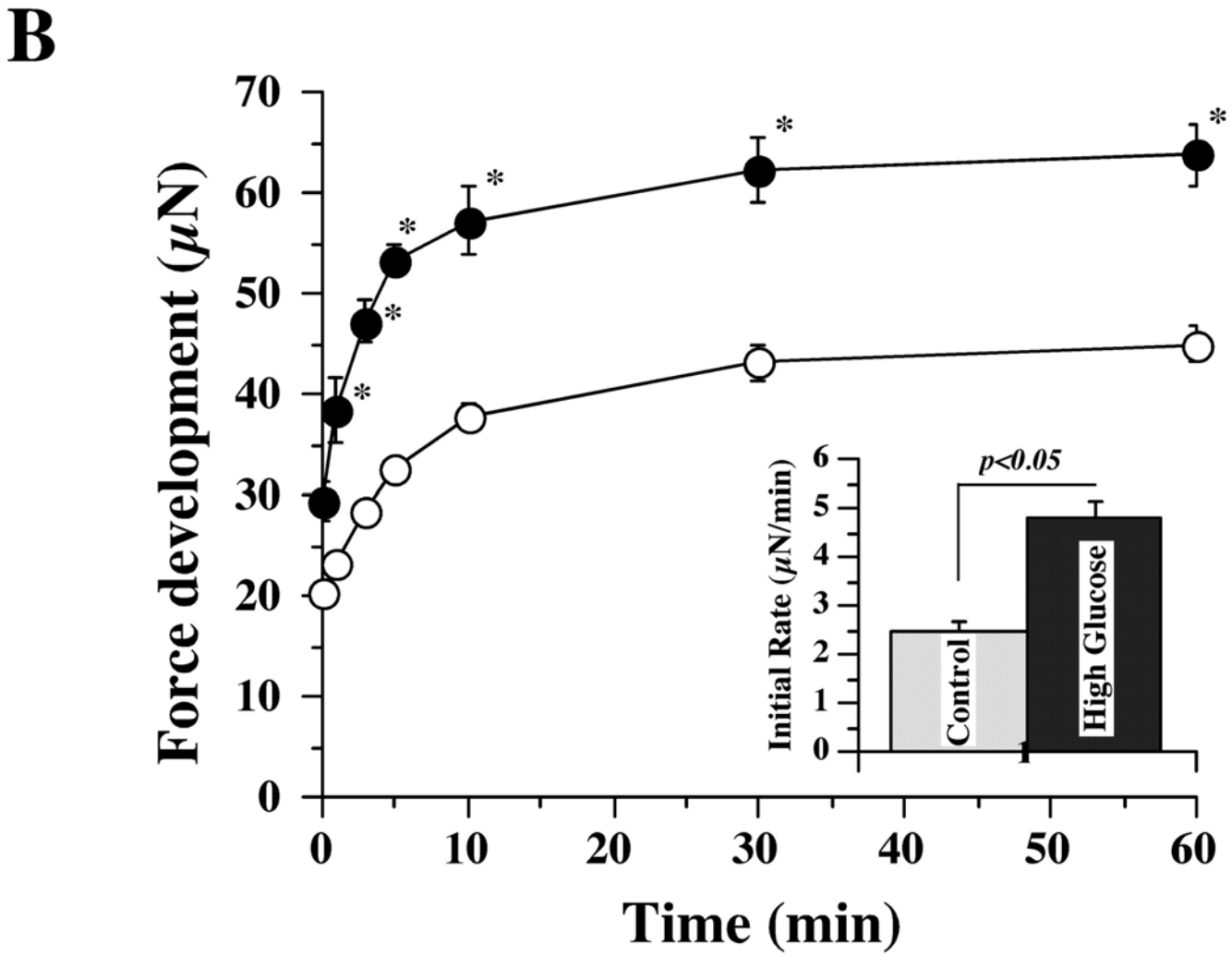

Figure 3

JPET Fast Forward. Published on May 12, 2006 as DOI: 10.1124/jpet.106.105015

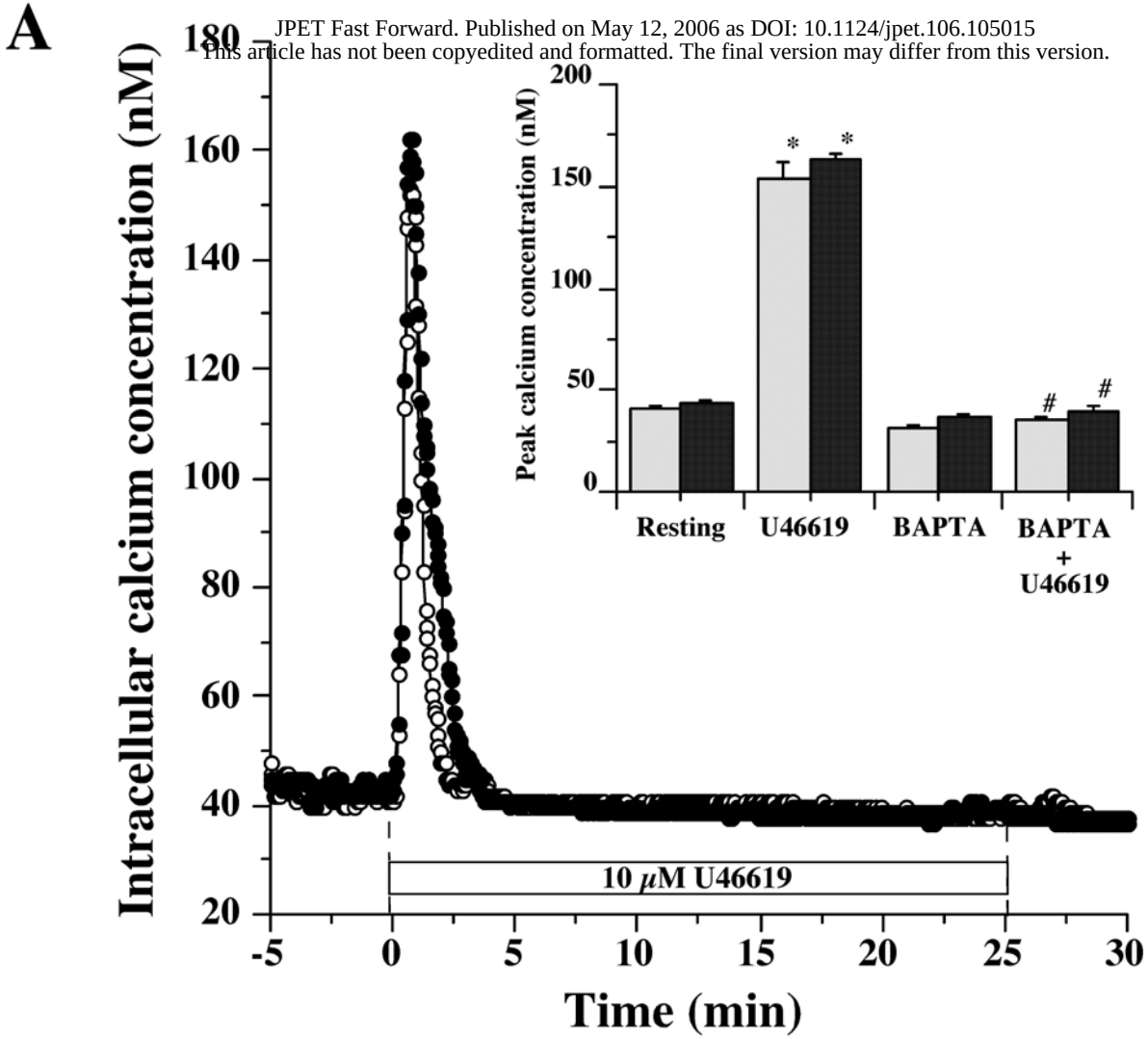

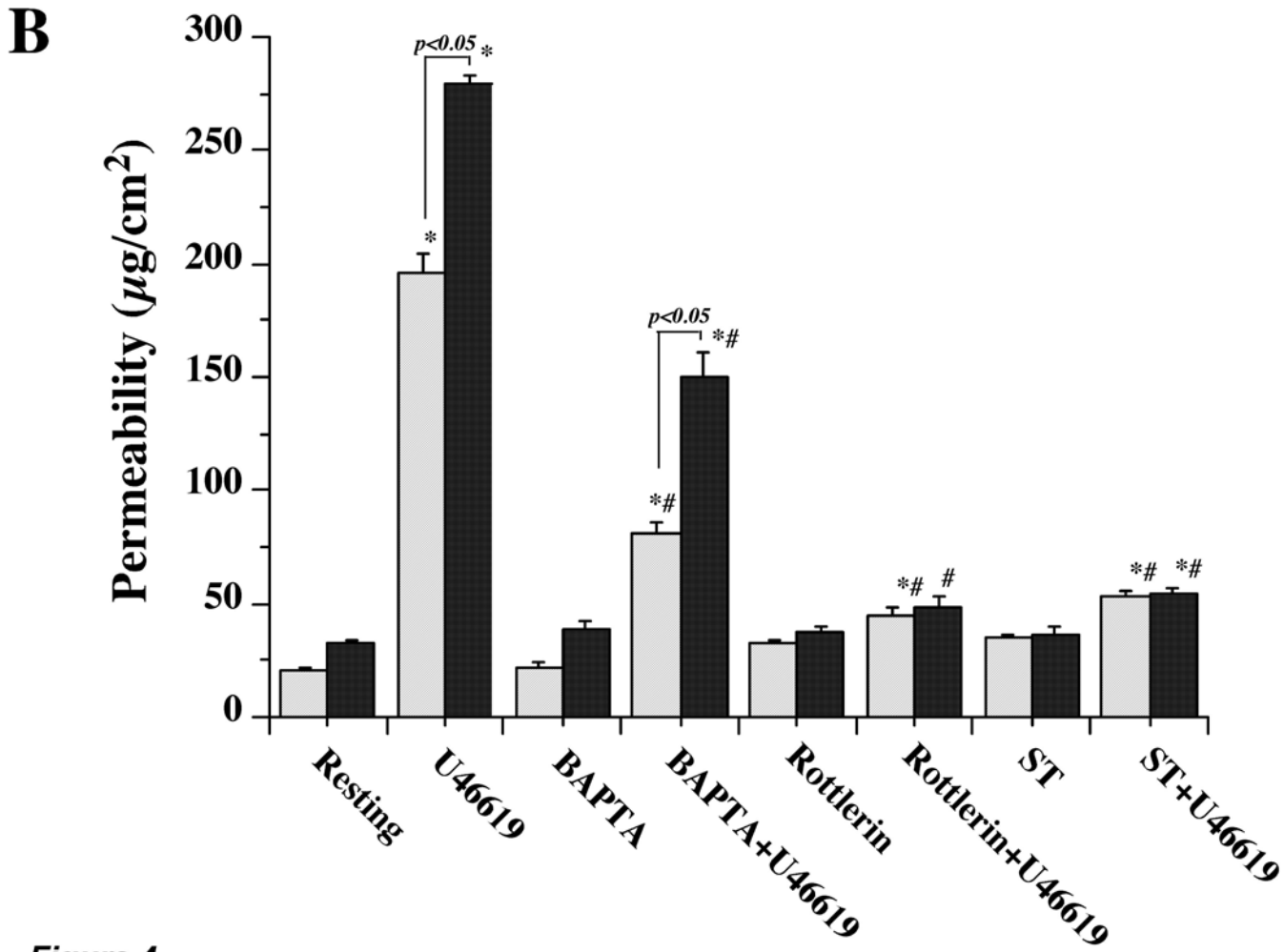

Figure 4

JPET Fast Forward. Published on May 12, 2006 as DOI: 10.1124/jpet.106.105015
This article has not been copyedited and formatted. The final version may differ from this version.

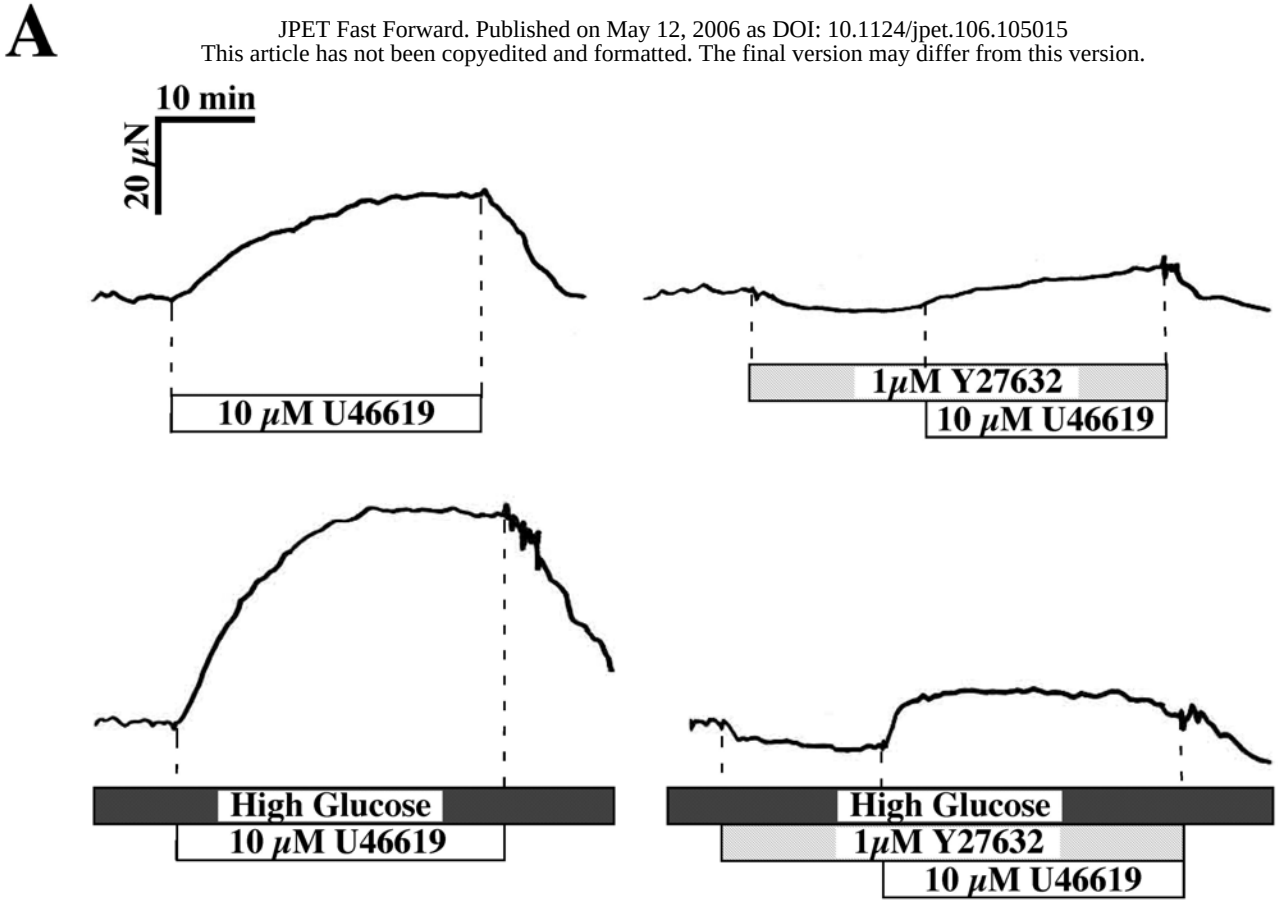

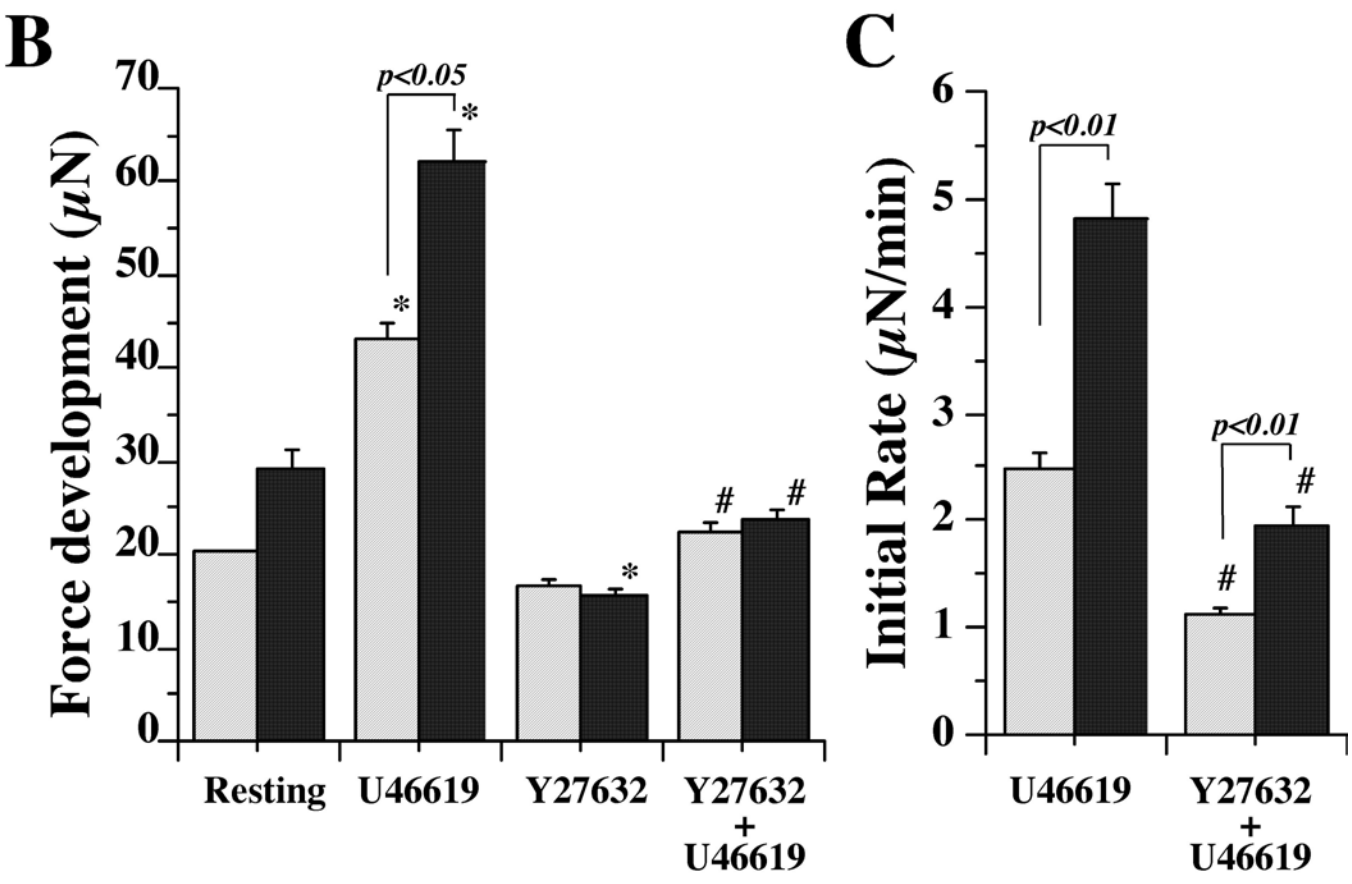

Figure 5A-5C

JPET Fast Forward. Published on May 12, 2006 as DOI: 10.1124/jpet.106.105015
This article has not been copyedited and formatted. The final version may differ from this version.

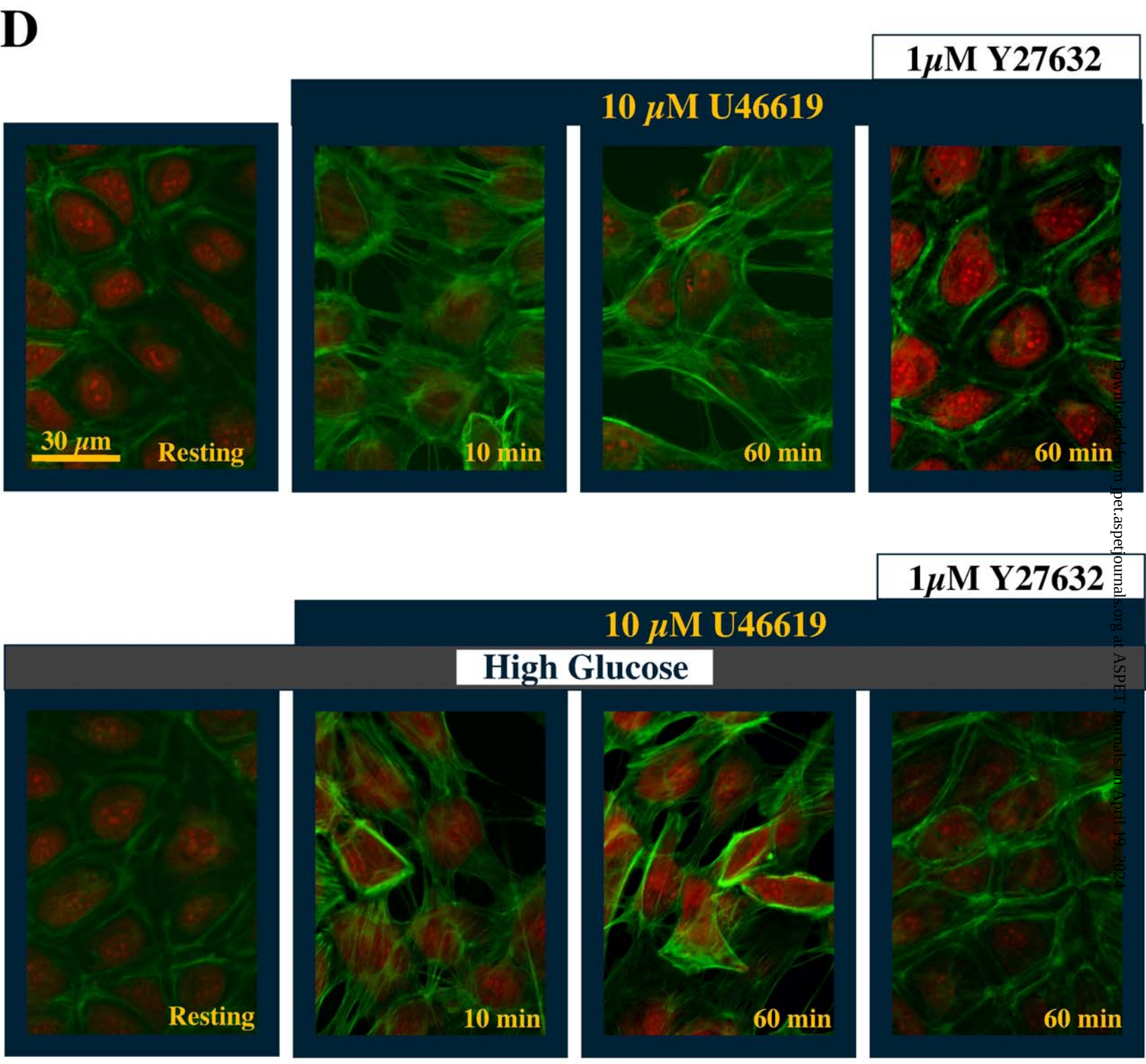

Figure 5D

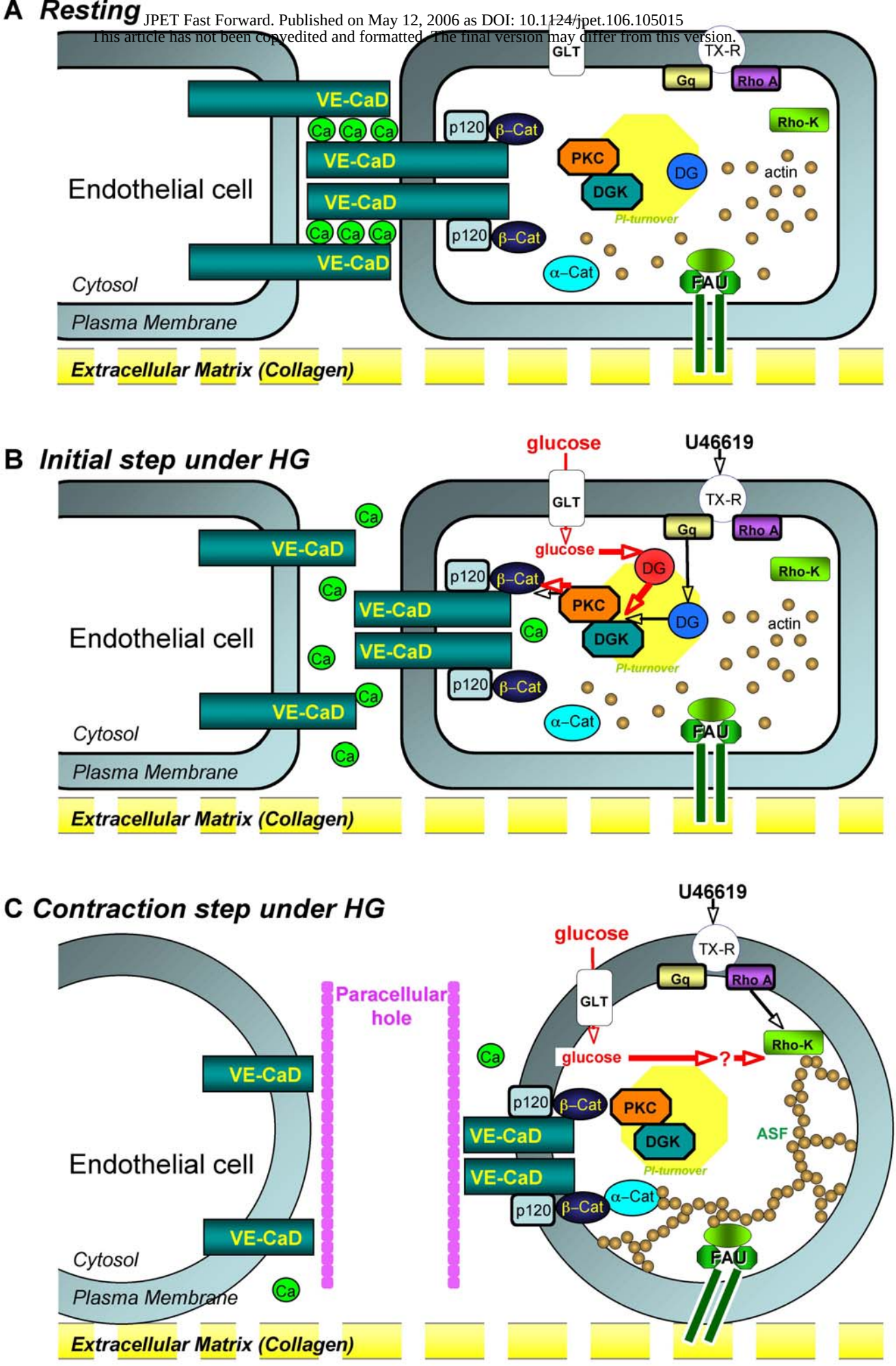

Figure 6